

CONTINUUM ACCELERATION OF BLACK HOLE WINDS

JOHN E. EVERETT AND DAVID R. BALLANTYNE

Canadian Institute for Theoretical Astrophysics, University of Toronto, 60 St. George Street, Toronto, ON M5S 3H8, Canada

Accepted to ApJL

ABSTRACT

Motivated by recent observations of high-velocity, highly ionized winds in several QSOs, models of purely continuum-driven winds launched from $\sim 200 GM_{\text{BH}}/c^2$ are presented. Launching conditions are investigated, as well as the observational signatures for a variety of initial conditions and illuminating continua. While we verify that continuum-driven, highly-ionized outflows reach the observed velocities for $L/L_{\text{Edd}} \geq 1$, independent of the incident spectral shape, such winds are too highly ionized to exhibit the observed absorption features when launched with an AGN continuum (in fact, such winds are so ionized that they are driven primarily by electron scattering). If the wind is instead illuminated with a blackbody continuum originating from an optically thick shield, the gas is too weakly ionized and does not produce high energy absorption features. If high-velocity, high-ionization winds are truly launched from very near the black hole, such winds must be launched under other conditions or via other processes; we summarize some possibilities.

Subject headings: galaxies:active – quasars:absorption lines – accretion, accretion disks – galaxies:individual (PG 1211+143) – X-rays:galaxies

1. INTRODUCTION

Optical, UV, and X-ray absorption troughs in Active Galactic Nuclei (AGN) spectra are central to the ongoing effort to understand not only mass outflow in AGN, but to provide clues to the fueling of their central supermassive black holes (see Crenshaw, Kraemer, & George 2003). Although the optical depth, metallicity, and velocity of such outflows are becoming increasingly well-constrained, the mechanism accelerating the winds remains elusive: thermal (e.g., Krolik & Kriss 1995), continuum-driven (for instance, Chelouche & Netzer 2003), line-driven (e.g., Murray et al. 1995; Proga, Stone, & Kallman 2000), and hydromagnetic (e.g., Königl & Kartje 1994; Bottorff et al. 1997) winds may all provide insight, but none of the above models have been excluded or are definitively observationally preferred for AGN outflows.

In this Letter, observational constraints on continuum-driven winds launched from very near the central black hole are examined. Such wind models have become significant, as observations of outflows apparently moving at large fractions of the speed of light ($v \sim 0.1$ – $0.4c$) have been published by Chartas, Brandt & Gallagher (2003), Chartas et al. (2003), Pounds et al. (2003a,b), and Reeves, O’Brien, & Ward (2003). From the measured high velocities, the winds are inferred to be launched very close to the central black hole. King & Pounds (2003) have proposed that the highly-ionized gas is subject to continuum driving near the central black hole because line driving is unlikely to be important for the large ionization parameters in these winds.

A model of a continuum-driven wind is presented in §2. This model is used to investigate terminal velocities and absorption features displayed by a variety of winds with different incident continua, initial shielding columns, and densities at the base of the wind (§3).

2. MODEL OVERVIEW

Electronic address: everett, ballantyne@cita.utoronto.ca

Our simple continuum-driven wind model consists of a radial streamline set to rise above the disk at a constant angle of 5° to the disk, with the initial column ($N_{\text{H},0}$) and number density (n_0) of the wind specified by the user. Gas with that initial density is assumed to be in Keplerian motion and is perturbed into the central, illuminating continuum with an initial velocity of roughly the local sound speed. To determine the gas’s motion due to continuum acceleration, Cloudy (Ferland 2002) simulations are run on a radial rays through the wind, spaced logarithmically in co-latitude. The continuum acceleration on the gas is then computed using both the ionization state and transmitted continuum (therefore taking account of any self-shielding effects) at the end of each radial slice through the wind, taking into account both electron scattering and bound-free opacities. The radiative acceleration is calculated and then compared to gravity in Γ_{cont} , defined as:

$$\Gamma_{\text{cont}} = \frac{a_{\text{cont}}}{g} = \frac{\frac{1}{\rho c} \int \chi_\nu F_\nu d\nu}{\frac{GM_{\text{BH}}}{R^2}} \quad (1)$$

where a_{cont} is the continuum radiative acceleration, g is the gravitational acceleration, ρ is the density in the wind, c is the speed of light, χ_ν is the frequency-dependent continuum opacity (output by Cloudy), F_ν is the transmitted continuum (again, given by Cloudy), G is the gravitational constant, M_{BH} is the mass of the central black hole, and R is the spherical radius. This Γ_{cont} factor is then input into the Euler equation along with the component of gravity and centrifugal acceleration along the radial flowline:

$$\frac{dv}{dr} = -\frac{GM_{\text{BH}}(1 - \Gamma_{\text{cont}})}{R^2} \cos(\theta - \theta_F) + \frac{v_\phi^2(\varpi)}{\varpi} \sin \theta_F \quad (2)$$

where ϖ is the cylindrical radius, θ is the co-latitude, θ_F is the (fixed) angle of the flowline from the vertical, and $v_\phi(\varpi) = \Omega_0 r_0^2 / \varpi$ is the azimuthal velocity (angular momentum is conserved in outflowing gas).

We integrate this equation to compute the velocity of the wind as a function of distance along the radial streamline. As that velocity increases, the number density in the wind (as well as the column density) decreases via mass conservation. For the first set of Cloudy simulations, where no velocity

data are available, the density is set to fall as r^{-2} ; this initial density distribution is replaced in subsequent iterations and is unimportant for the final results. The solution is iterated at least twice to ensure that the density structure is consistent with the velocity profile in the wind; simulations in test cases have shown that the wind structure does not change after two iterations, even when ten iterations are completed.

The wind parameters chosen in this paper reproduce the observational constraints on the outflow observed by Pounds et al. (2003a) in the narrow emission line quasar PG 1211+143. They observed an outflow with $v \sim 0.08c$ and an inferred density of $n \sim 3 \times 10^8 \text{ cm}^{-3}$, situated at $3 \times 10^{15} \text{ cm}$ from the black hole (this density is estimated observationally from the emission measure and line-of-sight column density; see Pounds et al. 2003a). They also inferred a launching radius of $r_0 = 10^{15} \text{ cm}$ by noting that $v = 0.08c \sim v_{\text{esc}}$, the escape velocity for that r_0 . Since $\dot{M} = 4\pi br^2 \rho v$ (where b is the covering factor of the flow, r is the radial distance, ρ is the mass density, and v the velocity of the wind) must be constant along the flow, an original density of $\sim 5 \times 10^{12} \text{ cm}^{-3}$ is inferred for the base of the wind if the initial velocity is of order 20 km/s and $b = 0.8$ (the value of b used in Pounds et al. 2003a). Observations indicate that $M_{\text{BH}} \approx 4 \times 10^7 M_{\odot}$ (Kapsi et al. 2000)¹, and $L_{\text{Edd}} \approx 5 \times 10^{45} \text{ erg/s}$ ($L/L_{\text{Edd}} \sim 0.8$ as the “Big Blue Bump” that dominates the continuum in PG 1211+143 has $L \sim 4 \times 10^{45} \text{ erg/s}$; Pounds et al. 2003a). The inferred mass outflow rate from the observations is $\sim 2.8 M_{\odot}/\text{yr}$ (for the covering fraction $b = 0.8$). We assume solar abundances.

The increase of density towards the base of the wind (where the gas is outflowing much more slowly) results in a large increase in the column density over the observed column of $\sim 5 \times 10^{23} \text{ cm}^{-2}$. As recognized by King & Pounds (2003), this column would be significantly optically thick, precluding photoionization simulations. Two possibilities are therefore considered in our simulations. First, “standard” winds are tested with $N_{\text{H},0} < 10^{24} \text{ cm}^{-2}$ at the base of the outflow and with an AGN spectral energy distribution (SED). Next, winds are launched by a soft X-ray/UV blackbody from the photosphere of an optically thick shield, as hypothesized by King & Pounds (2003).

3. KINEMATICS AND ABSORPTION FEATURES

The most immediate check for these outflows is to see which parameters lead to the observed velocities. Figure 1 displays v_{∞} as a function of the Eddington ratio (v_{∞} here is the velocity at the end of the model’s streamline at a distance of $100r_0$ where r_0 is the launch radius of our wind; taking the terminal velocity at $10^4 r_0$ only changes v_{∞} by $\sim 1\%$ in tests). This figure shows the variation in v_{∞} for both an AGN SED (Risaliti & Elvis 2004)² and for a blackbody continuum with a range of temperatures (as proposed by King & Pounds 2003). As a simple starting case, the winds presented here are optically thin, with $N_{\text{H},0} = 10^{22} \text{ cm}^{-2}$; higher columns are considered below.

As expected, when $L/L_{\text{Edd}} < 1$, the wind does not reach $v_{\text{obs}} \sim v_{\text{esc}}$, even with the added bound-free opacity used to calculating the continuum acceleration. For $L/L_{\text{Edd}} \geq 1$,

¹ A recent reanalysis by Peterson et al. (2004) yields $1.46 \pm 0.44 \times 10^8 M_{\odot}$ (with significant uncertainty noted in the analysis); we retain the value of $4 \times 10^7 M_{\odot}$ to compare with previous models.

² The Risaliti & Elvis (2004) spectrum is approximated by using Cloudy’s “AGN” continuum with the Big Blue Bump peaking at $T = 1.5 \times 10^5 \text{ K}$, $\alpha_{\text{OX}} = -1.43$, $\alpha_{\text{UV}} = -0.44$, $\alpha_{\text{X}} = -0.9$.

winds can achieve the observed velocities. Figure 1 clearly shows that the blackbody continuum can also accelerate a wind, resulting in almost identical velocities as when the Risaliti & Elvis (2004) SED is used. This seems reasonable since the majority of Γ_{cont} is given by frequency-independent electron scattering.

Next, to test the sensitivity of these results to initial parameters, both the column and the initial density of the wind are varied (see Fig. 2) for winds illuminated with the AGN SED from Risaliti & Elvis (2004). This shows that changing the initial density by an order of magnitude (which increases \dot{M} by the same factor) does not change the velocity structure of the wind significantly, due to the fact that the continuum is strong enough to highly ionize both winds. For such highly-ionized continuum driven winds, the degree of acceleration is governed by n_e/ρ which is nearly identical for both winds (although the higher-density wind does have a lower ionization parameter near the base of the wind, yielding larger accelerations there than in the lower-density wind).

Also in Figure 2, the shielding column at the base of the wind is varied from the normal $N_{\text{H},0} = 10^{22} \text{ cm}^{-2}$ to $N_{\text{H},0} = 5 \times 10^{23} \text{ cm}^{-2}$ to investigate the “self-shielding” of a thicker wind. This thicker column also does not change the final velocities in the outflow.

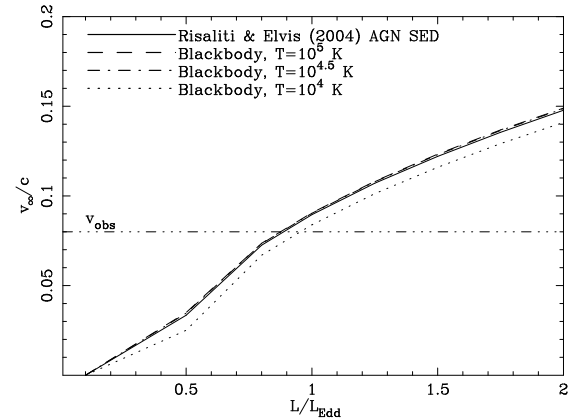


FIG. 1.— The final velocity of continuum-driven wind models as a function of the Eddington ratio of the central continuum for a range of incident SEDs. For continuum driving in such highly ionized sources, the final velocity is relatively independent of the SED. The observed velocity of $v_{\text{obs}} = 0.08c$ in PG 1211+143 is shown for comparison. Note that, for $L/L_{\text{Edd}} \lesssim 1$, winds do not escape the system, but we plot their velocities at $s = 100r_0$ to show the trend as L/L_{Edd} increases.

These figures address the range of Eddington ratios necessary to launch a wind to the observed velocity. But what are the particular spectral signatures of such a wind? To answer this question, Figures 3 and 4 show the X-ray ionization parameter, ξ , as a function of L/L_{Edd} for those different models. We define ξ in the same manner as Cloudy and XSTAR: $4\pi F_{\text{X}}/n_{\text{H}}$, where F_{X} is the integrated X-ray flux from 1 to 1000 Rydbergs. To pick one ‘fiducial’ ξ out of the range of ionization parameters in the accelerating wind, ξ is extracted at a distance along the flow of $s = 3r_0$ (chosen to compare with the inferred distance of the wind in PG 1211+143).

Figures 3 and 4 display the ionization parameters in these continuum-driven winds. They show that the high velocity, continuum-driven winds must by necessity have been accelerated by a large incident flux, which, for AGN-like continua, leads to extremely high ionization parameters in the wind (ξ

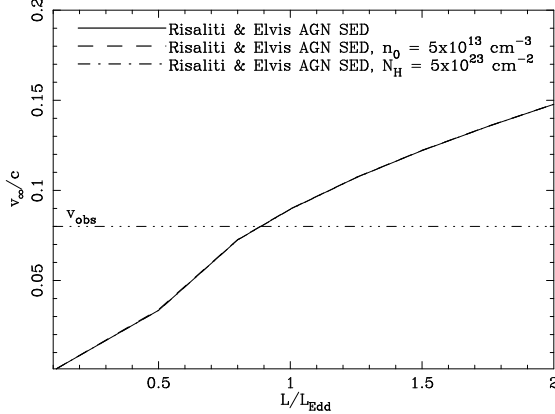


FIG. 2.— The final velocity of continuum-driven wind models vs. L/L_{Edd} for the Risaliti & Elvis (2004) incident spectrum with changes to the initial density and initial wind column. Unless otherwise noted in the legend, the models have $N_{\text{H},0} = 10^{22} \text{ cm}^{-2}$ and $n_0 = 5 \times 10^{12} \text{ cm}^{-3}$. Neither the increased initial column nor density affect the wind significantly. The observed velocity of $v_{\text{obs}} = 0.08c$ in PG 1211+143 is shown for comparison.

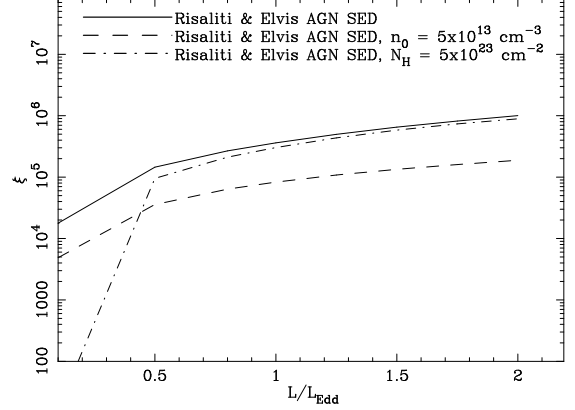


FIG. 4.— As in Fig. 3, but using the Risaliti & Elvis (2004) continuum to investigate variations in density and shielding. Unless otherwise noted in the legend, the models have $N_{\text{H},0} = 10^{22} \text{ cm}^{-2}$ and $n_0 = 5 \times 10^{12} \text{ cm}^{-3}$. The larger density wind yields a somewhat smaller ξ , even though it experiences a very similar acceleration to the lower-density model. The $N_{\text{H},0} = 5 \times 10^{23} \text{ cm}^{-2}$ wind has a very similar ionization parameter for $L/L_{\text{Edd}} \geq 1$.

of order $10^5 - 10^6$ for $L/L_{\text{Edd}} \geq 1$). The $T = 10^5 \text{ K}$ blackbody spectrum also has a very high ionization parameter, but all of its energy in the 1-1000 Rydberg window is concentrated near 1 Rydberg. Thus, even though this continuum has a large ionization parameter, the lack of X-ray photons means that the ionization stages within the gas are much lower than that produced by an AGN SED: for instance, the predominant state of iron for the wind illuminated by the $T = 10^5 \text{ K}$ blackbody spectrum is Fe IX, while the observed iron ions are Fe XXV and Fe XXVI (Pounds et al. 2003a).

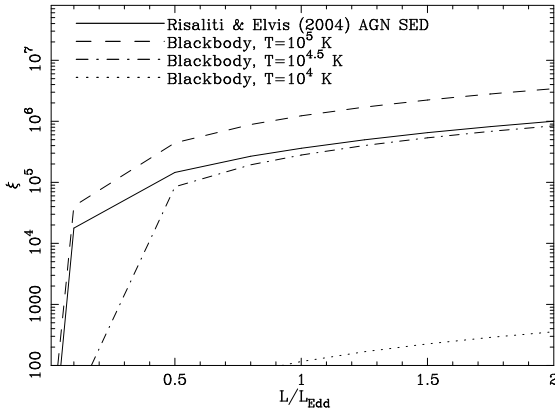


FIG. 3.— The X-ray ionization parameter, ξ , as a function of L/L_{Edd} for a range of incident continua at the inferred location of the absorbing gas in PG 1211. The relative values of the ionization parameter are set by the amount of flux each SED has in the range of 1 to 1000 Rydbergs, where ξ is calculated. The AGN SED yields ionization parameters too high to explain the observed line absorption. While the blackbody continua can have relatively high ionization parameters, they have no flux in the X-ray regime to ionize iron to the states observed in PG 1211+143.

This has important implications for observations of such winds. King & Pounds (2003) postulated that continuum driven winds could account for high-velocity X-ray absorption features. As mentioned in the introduction, there have been other recent observations of such high-velocity X-ray absorption in a variety of QSOs (Chartas, Brandt & Gallagher 2003; Chartas et al.

2003; Pounds et al. 2003b; Reeves, O'Brien, & Ward 2003). In observations of PG 1211+143, significant equivalent widths (EWs) for absorption features in Mg XII, S XVI, Fe XXV, and Fe XXVI are seen. Table 1 compares these observations to models of a high-column wind with an AGN SED (Risaliti & Elvis 2004), $N_{\text{H},0} = 5 \times 10^{23} \text{ cm}^{-2}$, assumed line widths of 1000 km/s (Pounds et al. 2003a) and $L/L_{\text{Edd}} = 1$. Equivalent widths are calculated in the linear weak line limit:

$$W_{\text{eV}} = \Delta E_D \sqrt{\pi} \tau_0 \times [1 - \tau_0 / (2! \sqrt{2}) + \tau_0^2 / (3! \sqrt{3}) + \dots] \quad (3)$$

for $\tau_0 \lesssim 1$, where τ_0 is the optical depth in the line from Cloudy and ΔE_D is the Doppler width of the line in eV (all of the lines shown here have $\tau_0 \lesssim 1$ in the wind). A comparison of observed EWs to the model EWs clearly shows that, because of the high ionization in the outflow, such winds cannot account for the EWs observed in PG 1211+143. The EWs for winds illuminated with a blackbody spectrum are even smaller, although in that case the small EWs are due to the lack of high-energy ionizing X-rays.

To test the particular parameters presented by Pounds et al. (2003a), we assembled a model with a constant column of $N_{\text{H}} = 5 \times 10^{23} \text{ cm}^{-2}$ present throughout the wind. Although the density still declines with height above the disk as before, we set the column to a constant value for every line of sight through the wind. This would therefore yield the column of $N_{\text{H}} = 5 \times 10^{23} \text{ cm}^{-2}$ at $s = 3r_0$ as observed by Pounds et al. (2003a). This model differs strongly from the other solutions where the column drops consistently as the density in the wind falls. The last column of Table 1 displays the EWs from this model with $L/L_{\text{Edd}} = 1$; at higher L/L_{Edd} , the EWs only decrease. Even with the constant column supplying a greater column of the relevant ions, the ionization parameter in the model is so high that the line equivalent widths fall below the 90% confidence interval of the measurements.

We have searched for some area of parameter space that might allow such continuum-driven winds to show the observed equivalent widths. The only possibility we have found is modifying the incident continuum such that $\alpha_x = -2$ ($\Gamma = 3$). While inconsistent with the observed power law of $\Gamma \sim 1.75$, this does yield equivalent widths consistent with

TABLE 1
COMPARISON OF EQUIVALENT WIDTHS FOR PG 1211+143 (FROM POUNDS ET AL. 2003A) TO A CONTINUUM DRIVEN WIND.

| Line | Observed EW [eV] ^a | Model EW [eV] ^b $N_{\text{H},0} = 5 \times 10^{23} \text{ cm}^{-2}$ | Model EW [eV] ^{bc} $N_{\text{H}} = 5 \times 10^{23} \text{ cm}^{-2}$ |
|---------------------|-------------------------------|---|--|
| Fe XXVI Ly α | 95 \pm 20 | 7×10^{-4} | 31 |
| Fe XXV 1s-3p | 45 \pm 12 | 2×10^{-5} | 0.2 |
| Fe XXVI Ly β | 45 \pm 12 | 1×10^{-3} | 8 |
| S XVI Ly α | 32 \pm 12 | 2×10^{-4} | 1.4 |
| Mg XII Ly α | 15 \pm 6 | 6×10^{-5} | 0.4 |

^aErrors listed correspond to 90% confidence intervals.

^bEquivalent widths are those found at $s = 3r_0$, the inferred location of the sight-line through the outflow in PG 1211+143.

^cThe column for this calculation is held constant throughout the outflow, unlike all previous models, to compare with Pounds et al. (2003a).

the observations for all lines except Fe XXV, but only for the wind with constant column of $N_{\text{H}} = 5 \times 10^{23} \text{ cm}^{-2}$ along the entire outflow. However, in the rather implausible case that the X-ray continuum is formed outside the wind (so that the wind sees a different X-ray continuum than is observed), such a model does reproduce the observed equivalent widths.

As a final consideration, we note that for a large outflow with covering factor $b = 0.8$, P-Cygni profiles should be observed, but emission is not seen with the observed absorption lines. This may perhaps indicate a smaller covering fraction for the wind.

4. SUMMARY

This Letter addresses observational constraints on winds launched from near the central black hole of AGNs using pure continuum driving. This has become an increasingly significant topic very recently, with the observation of high-velocity, very highly ionized gas in several different QSOs, where the outflow is most likely too highly ionized to allow for significant line driving. As expected, continuum driving can accelerate highly-ionized winds from near the central black hole to the observed velocities when $L/L_{\text{Edd}} \geq 1$. But the models also indicate that:

1. Changes in the initial density or shielding column do not affect the final velocity of the wind. Nor do changes in the illuminating continuum significantly change the final velocities in the wind, although moving to softer continua does significantly lower the ionization state.
2. Continuum-driven winds, illuminated by an AGN SED and accelerating to the observed velocities quickly become very highly ionized (with $\xi \sim 10^5 - 10^6$ for

$L/L_{\text{Edd}} \geq 1$), completely stripping the outflowing gas, resulting in acceleration primarily by electron scattering. Continuum-driven winds can be launched by blackbody SEDs but such outflows do not have the observed high-ionization lines.

3. Taking the particular example of the outflow observed in PG 1211+143 (Pounds et al. 2003a), wind models display much smaller EWs than the observed EWs. Softening the X-ray power law to $\Gamma \sim 3$ can increase the EWs, however this requires both a non-standard AGN continuum and a constant-column disk wind.

If pure continuum driving has difficulty reproducing the observations, what process is accelerating the wind? First, perhaps the wind is not relativistic (see Kaspi 2004, who finds the low-energy X-ray spectrum of PG 1211+143 to be consistent with a 3000 km/s outflow). It may also be possible that line-driving is playing a role, although such acceleration would have to occur only at the very base of the wind, where the ionization parameter is suitably low and where radiative launching would be difficult given the high column to the central source near the disk (but see Proga & Kallman 2004). Another option for explaining these outflows is a multi-phase wind, although such a wind would increase the mass outflow rate beyond its already large value.

Another possibility is that such high-velocity, highly-ionized winds could be launched hydromagnetically. The addition of hydromagnetic driving would decouple the ionization state from the acceleration process; instead of requiring, as for continuum-driven flows, that the luminosity be L_{Edd} or greater (which leads to over-ionization), the wind could possibly be accelerated by MHD forces that would allow a lower L/L_{Edd} and a lower ionization state. Indeed, a lower L/L_{Edd} may already be indicated by the larger M_{BH} (albeit with large uncertainty) found by Peterson et al. (2004). MHD wind models will be addressed in a subsequent paper, but we point out that the large mass outflow rates ($\gtrsim M_{\text{Edd}}$) inferred in this source may be too high for an MHD outflow. Model predictions for winds driven by all of the above processes will be useful in determining which forces are capable of launching these outflows and which model outflows are consistent with the observational signatures.

We thank the referee for helpful comments that improved the paper, and Doron Chelouche, Arieh Königl, & Norm Murray for their comments. This work is supported by the Natural Sciences and Engineering Research Council of Canada.

REFERENCES

Bottorff, M., Korista, K.T., Shlosman, I., & Blandford, R.D. 1997, ApJ, 479, 200
 Chartas, G., Brandt, W.N., & Gallagher, S.C. 2003, ApJ, 595, 85
 Chartas, G., Brandt, W.N., Gallagher, S.C., & Garmire, G.P. 2002, ApJ, 579, 169
 Chelouche, D., & Netzer, H. 2003, MNRAS, 344, 233
 Crenshaw, D.M., Kraemer, S.B., & George, I.M. 2003, ARA&A, 41, 117
 Ferland, G.J. 2002, Hazy, a Brief Introduction to Cloudy, University of Kentucky Department of Physics and Astronomy Internal Report
 Kaspi, S., Smith, P.S., Netzer, H., Maoz, D., Jannuzzi, B.T., & Giveon, U. 2000, ApJ, 533, 631
 Kaspi, S. 2004, in The Interplay among Black Holes, Stars, and the ISM in Galactic Nuclei, eds. Th. Shorchi Bergmann, L.C. Ho, & H.R. Schmitt, astro-ph/0405563
 King, A.R., & Pounds K.A. 2003, MNRAS, 35, 657
 Königl, A., & Kartje, J.F. 1994, ApJ, 424, 446
 Krolik J.H., & Kriss G.A. 1995, ApJ, 447, 512
 Murray N., Chiang J., Grossman S.A., & Voit G.M. 1995., ApJ, 451, 498
 Peterson, B. et al. 2004, Accepted to ApJ, astro-ph/0407299
 Pounds, K.A., Reeves, J.N., King, A.R., Page, K.L., O'Brien, P.T., & Turner, M.J.L. 2003, MNRAS, 345, 705
 Pounds, K.A., King, A.R., Page, K.L., & O'Brien, P.T. 2003, MNRAS, 346, 1025

Proga, D., & Kallman, ApJ accepted (astro-ph/0408293)
Proga D., Stone J.M., & Kallman T.R., 2000, ApJ, 543, 686
Reeves, J.N., O'Brien, P.T., & Ward, M.J. 2003, ApJ, 593, L65
Risaliti, G., & Elvis, M. 2004 in Supermassive Black Holes in the Distant Universe, ed. A.J. Barger (Dordrecht:Kluwer Academic Publishers), astro-ph/0403618